He et al. Supplemental Figure 1

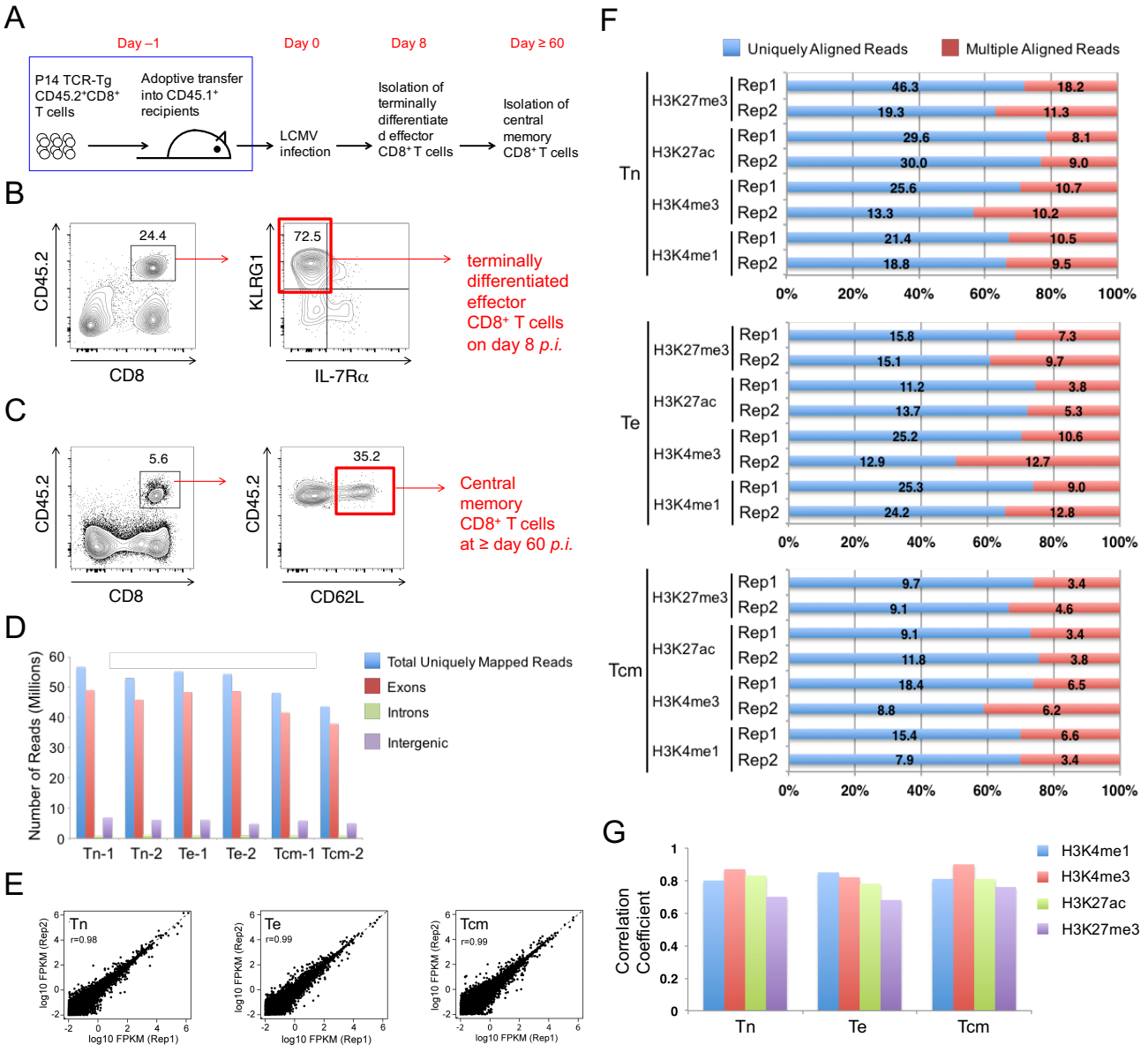

Figure S1 (related to Figure 1). Experimental design and quality assessment of the RNA-Seq and epigenomic data in CD8$^+$ T cell subsets.

(A) Generation of CD8$^+$ T cell subsets after viral infection. CD45.2$^+$ P14 TCR-Tg CD8$^+$ T cells were isolated from the lymph nodes, and 10,000 Tn cells were adoptively transferred into CD45 allele disparate, CD45.1$^+$ recipient mice. One day later, the recipient mice were intraperitoneally (*i.p.*) infected with 2×10^5 PFU of LCMV-Armstrong. On day 8 post-infection (*p.i.*), CD45.2$^+$CD8$^+$KLRG1$^+$IL-7Rα$^-$ cells were sort-purified as terminally differentiated effector CD8$^+$ T (Te) cells. On ≥ day 60 *p.i.*, CD45.2$^+$CD8$^+$CD62L$^+$ cells were purified as central memory CD8$^+$ T (Tcm) cells.

(B) Gating strategy for the purification of CD45.2$^+$CD8$^+$KLRG1$^+$IL-7Rα$^-$ Te cells.

(C) Gating strategy for the purification of CD45.2$^+$CD8$^+$CD62L$^+$ Tcm cells.

(D) Mapping statistics of RNA-Seq data. Sequencing reads were mapped to the mouse genome (release mm9) using Tophat. Uniquely mapped reads and their distribution across genomic regions in each sample were plotted.

On average, we obtained a sequence depth of 83.8 million reads per sample, of which 51.8 million reads were uniquely mapped.

(E) Reproducibility of RNA-Seq data**.** The FPKM values (fragments per kilo base of exonic sequence per million reads) for all transcripts were determined, and their distributions between two biological replicates were plotted. r, Pearson correlation coefficient.

(F) Mapping statistics of histone modification ChIP-Seq data. ChIP-Seq of indicated histone marks in Tn, Te, and Tcm cells were mapped to mouse genome (mm9) using Bowtie. The number and percentage of uniquely and multiply aligned reads are shown.

(G) Reproducibility of replicate ChIP-Seq samples. Shown is the Pearson correlate coefficient of two biological replicates for each histone mark ChIP-Seq.

He et al. Supplemental Figure 2

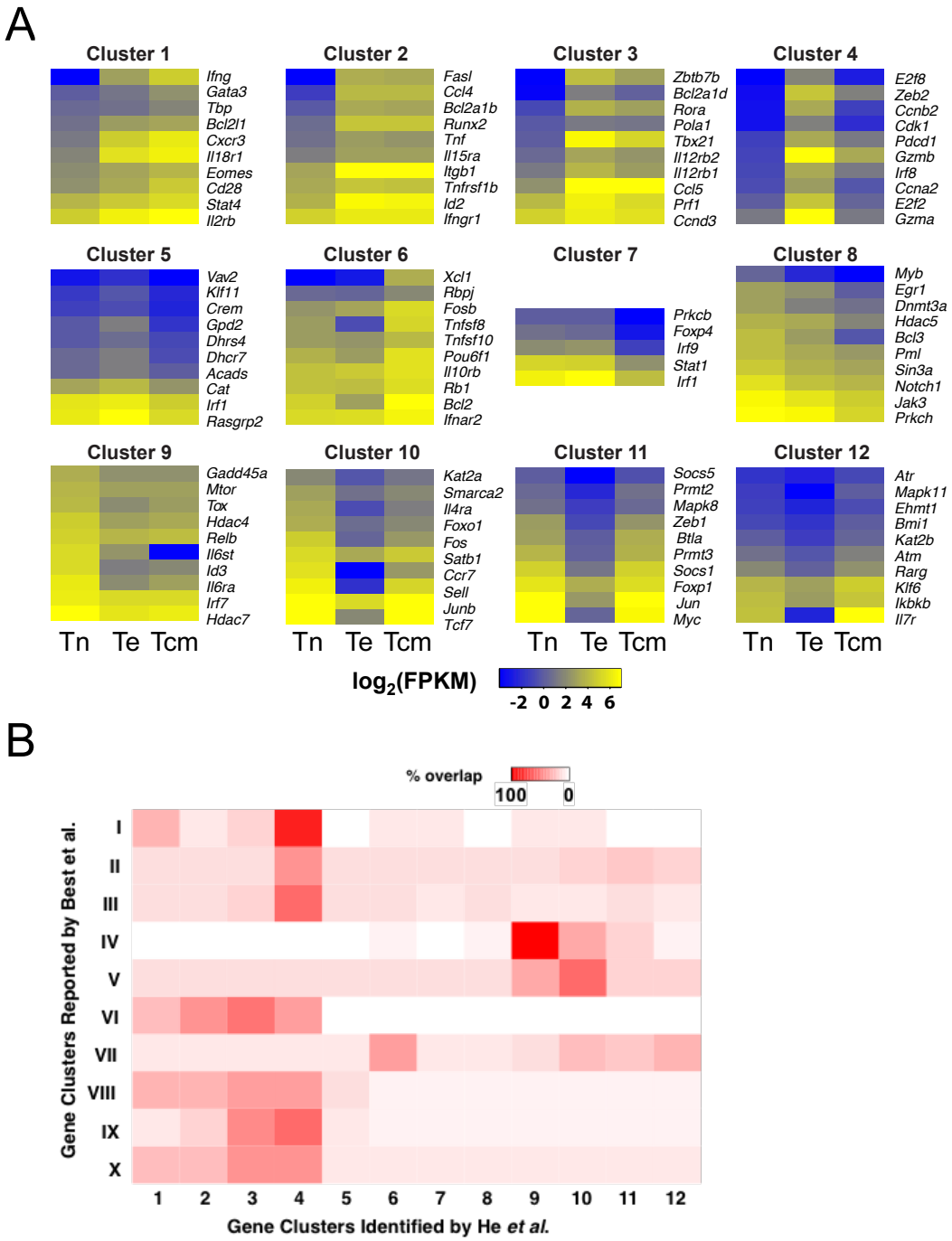

Figure S2 (related to Figure 1). Gene expression clusters (ExprCluters) defined in this study and their overlap with expression clusters defined in a previous microarray study.

(**A**) Representative genes in each ExprCluster. The FPKM values of select genes from each ExprCluster were log2-transformed and used to generate heatmaps. Selection of representative genes was based on their known or potential regulatory roles in $CD8^+$ T cell responses, as highlighted below.

Genes in clusters 1-3 retained elevated expression in Tcm compared to Tn, although compared with that of Te, their expression in Tcm is higher (ExprCluster 1), similar (ExprCluster 2) or lower (ExprCluster 3). These

clusters included well-characterized genes as well as potential novel regulators during Te differentiation and Tcm maturation. These genes include 1) transcriptional factors (TFs), such as Eomes, T-bet (*Tbx21*), Id2, and Thpok (*Zbtb7b),* Gata3, Stat4, Runx2, and RAR-related orphan receptor α (*Rora*); 2) cytotoxic effector genes such as FasL and perforin (*Prf1*); 3) regulators of cell survival such as Bcl-X_L (*Bcl2l1*), Bcl2-related A1 proteins (*Bcl2a1b* and *Bcl2a1d*); 4) cytokines and cytokine receptors, such as IFN-γ, TNF, IFN-γ receptor α chain (*Ifngr1*), TNF receptor 2 (*Tnfrsf1b*), IL-2 receptor β chain (*Il2rb*), IL-15 receptor α chain (*Il15ra*), IL-12 receptor β chains (*Il12rb1* and *Il12rb2*) and IL-18 receptor 1 (*Il18r1*); and 5) chemokines and chemokine receptors, such as Ccl4, Ccl5 and CXCR3.

After transient induction in Te, the expression of genes in clusters 4 and 5 in Tcm was reverted to a level similar to or lower than Tn. Genes in these clusters included granzymes (*Gzma* and *Gzmb*), and were enriched for regulators of cell cycle progression such as E2F family proteins (*E2f2* and *E2f8*), cyclins (*Ccna2* and *Ccnb2*) and cyclin-dependent kinase 1 (*Cdk1*), which is consistent with the proliferative bursts required for the massive Te expansion.

ExprClusters 6 and 7 contained genes that were not differentially expressed during Tn to Te transition, but up-regulated and down-regulated in Tcm, respectively. The up-regulated genes included Xcl1 and Bcl2, consistent with their specific regulatory roles as previously suggested (*Best et al. Nat. Immunol. 14, 404, 2013*). In contrast, the down-regulated genes have not been reported thus far, including several TFs such as Stat1, Irf1, Irf9 and Foxp4.

All genes in ExprClusters 8-12 were down-regulated in Te, but had different fates in Tcm. Clusters 8 and 9 genes were further down-regulated or maintained at reduced expression levels similar to Te. These genes included TFs such as Myb, Egr1, Id3 and Tox, histone deacetylases (HDACs) including *Hdac4*, *Hdac5*, and *Hdac7* and other components of HDAC complexes such as Sin3a. The reduced expression of HDACs in Tcm may be associated with increased signal intensity of H3K27ac and its contribution to gene regulation in memory $CD8^+$ T cells.

After initial down-regulation in Te, genes in clusters 10-12 were restored in Tcm to levels that were lower than (ExprCluster 10), similar to (ExprCluster 11), or higher than (ExprCluster 12) Tn cells. These genes included well-known Tcm characteristic genes such as CD62L (*Sell*), CCR7 and IL-7 receptor α chain (*Il7r*), and known TFs that regulate Tcm function and maturation such Tcf1 (*Tcf7*) and Foxo1. Our data further suggested additional genes that may be involved in Tcm regulation, including 1) TFs in the AP1 family including Jun, Fos, and Junb; 2) Other TFs including Myc, Foxp1, Klf6, Retinoic acid receptor γ (*Rarg*); 3) chromatin remodeling genes such as BRM (*Smarca2*) and the genome organizer Satb1; 4) cytokine signaling pathways including IL-4 receptor α chain (*Il4ra*) and suppressor of cytokine signaling proteins (*Socs1* and *Socs5*); 5) DNA damage repair, including ATM, ATR, and Bmi1; and 6) epigenetic regulators, including histone acetyltransferases (HATs) such as *Kat2a* and *Kat2b*, histone arginine N-methyltransferases such as *Prmt2* and *Prmt3*, and histone lysine N-methyltransferase Ehmt1 which catalyzes H3K9 methylation.

(**B**) Comparison of our RNA-Seq-based ExprClusters with microarray-based expression clusters by *Best et al*.

Best *et al*. (*Nat. Immunol. 14, 404, 2013*) used expression microarray to profile $CD8^+$ T cell responses and identified 1,463 differentially expressed genes in 10 clusters. Among these, 1,026 genes (70.1%) overlapped with the 2,766 genes in our 12 ExprClusters. The level of overlap was shown as a percentage of all genes in each cluster using the indicated color scale.

[Additional notes]

The discrepancy between the two studies may be ascribed to the following:

1) As noted in the text, our study focused on more purified Te and Tcm subsets rather than bulk heterogeneous effector and memory $CD8^+$ T cells.

2) RNA-Seq is more sensitive in detecting low-abundance transcripts than microarray. Among all DEGs newly identified in this study (listed in **Table S2**), 1,074 of the 1,740 DEGs (68 %) had FPKM values ≤10, such as *Rxra* transcripts in ExprClusters 3 and 4, *Zfp281* in ExprCluster 10, and *Thra* transcripts in ExprClusters 10

and 11. In spite of their low abundance, our enhancer motif analyses identified these transcription factors as key regulatory nodes during the Tn, Te, and Tcm transition (**Figures 6** and **7**). In a large-scale survey of transcriptomes of 15 human cell types, it is observed that a range of gene expression spans six orders of magnitude for polyadenylated RNAs (10^{-2}-10^{4} FPKM) (*Djebali et al. Nature 489, 101, 2012*). Almost one-quarter of expressed protein-coding genes are present in the cells with a FPKM < 1. Therefore, genes with transcripts detected within 1-10 FPKM may be biologically important and are worthy of inclusion, so as to provide a more complete picture of transcriptomic changes during $CD8^+$ T cell responses.

3) The study by Best *et al*. included several early time points, *i.e*., 12, 24, and 48 hrs after $CD8^+$ T cell activation. Genes in our ExprClusters 1-4 (up-regulated in the fully differentiated Te) exhibited strong overlaps with their clusters I, II, and III (showing quick induction within 48 hr *p.i.*), clusters VI, IX, and X (showing delayed induction after 48 hr *p.i.*), and cluster VII (showing rather repression within 48 hr *p.i.*). Among the 437 genes that were not identified in our analysis (**Table S2**), 327 genes (75%) showed ≥1.4 fold increase and 67 genes (15%) showed ≥1.4 fold decrease in expression within 48 hours of activation.

4) Because many more time points were used in the clustering analysis by Best *et al*., their result may have missed genes that showed evident expression changes only at the peak Te and/or Tcm response stages. For examples, *Il2rb* (encoding IL-2Rβ), *Eomes*, and *Bcl2l1* (encoding Bcl-X_L) in ExprCluster 1, *Lef1* in ExprCluster 9, and *Foxo1* in ExprCluster 10 are known DEGs and contribute to regulation of $CD8^+$ T cell responses (*Hess Michelini et al., J. Exp. Med. 210, 1189, 2013; Intlekofer et al., Nat Immunol. 6, 1236, 2005; Kim et al., Immunity 39, 286, 2013; Song et al., J. Immunol. 175, 3534, 2005; Tejera et al., J. Immunol. 191, 187, 2013; Zhou and Xue, J. Immunol. 189, 2722, 2012),* but are not included in the 10 clusters reported by Best *et al*.

All DEGs newly identified in this study are functionally annotated in **Table S2**, with expression levels in both studies listed side-by-side for a direct comparison.

He et al. Supplemental Figure 3

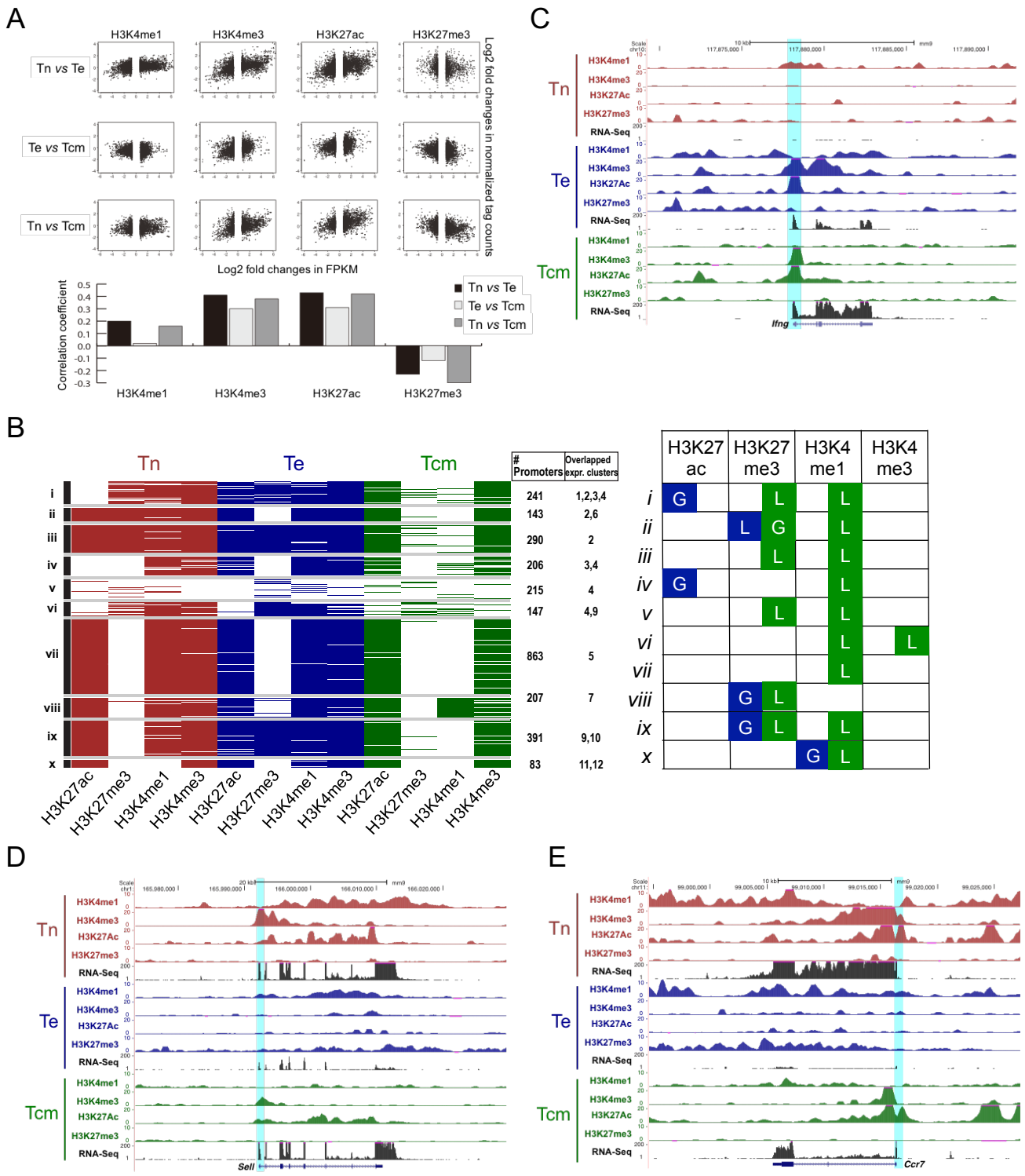

Figure S3 (related to Figure 1). Identification of epigenetic clusters at the promoters of differentially expressed genes (DEGs) during CD8$^+$ T cell responses.

(A) Correlation between histone modification signals at gene promoters and gene expression levels. The tag counts of each histone mark at each promoter (–5 kb to +1 kb flanking the TSSs) were determined for all DEGs

in **Figure 1A**. Promoter histone mark signal changes were plotted against gene expression changes for each pair-wise comparison among Tn, Te, and Tcm cells. Pearson correlation coefficients were shown in lower panel.

(B) Epigenetic clusters at promoters of DEGs. Histone modification profiles of promoters were clustered using Consensus Clustering. The size of each cluster and the overlapping ExprCluster(s) are shown to the right of the heatmap. Significance of overlap between ProEpi Clusters and ExprClusters was computed using the hypergenomic distribution with a p-value cutoff of 0.05.

Shown in the right panel is a graphical summary of histone modification changes at promoters between adjacent $CD8^+$ T cell response stages. Blue square, transition from Tn to Te; Green square, transition from Te to Tcm; G, gain of histone mark; L, loss of histone mark.

(C-E) Genome browser view of histone modification and expression profiles at *Ifng* (C), *Sell* (D) and *Ccr7* (E) gene loci. The gene structure and transcription orientation are marked at the bottom of each panel, and the promoter regions are highlighted in cyan.

[Additional notes]

By intersecting the ProEpi Clusters with ExprClusters defined in **Figure 1B**, we found consistent epigenetic features at the promoters associated with gene expression changes (**B**). The promoters of genes in ExprClusters 1-3 (up-regulated in Te and Tcm) were significantly enriched in ProEpi Clusters *i-iv,* sharing the common features of loss of H3K4me1 in Tcm, consistent with a reported repressive role of H3K4me1 at the gene promoters (*Cheng et al., Mol. Cell 53, 979, 2014*). These clusters also had gain of H3K27ac in Te, and/or loss of H3K27me3 in Te or Tcm (**B**). For an example, the *Ifng* gene (in ExprCluster 1, ProEpi Cluster *i*) showed gain of H3K27ac in both Te and Tcm and subsequent loss of H3K27me3 in Tcm, which presumably allowed its sustained increased expression (**C**). On the other hand, the promoters of genes in ExprClusters 9-12 (down-regulated in Te but expressed at various levels in Tcm) were enriched in ProEpi Clusters *ix* and *x*. These clusters showed gain of H3K27me3 or H3K4me1 in Te cells accompanied by consistent loss of H3K4me1 in Tcm cells (**B**), which may contribute to gene down-regulation at the effector phase and partially restored expression at the memory phase. *Sell* and *Ccr7* (in ExprCluster 10, ProEpi Cluster *ix*) are two such examples (**D** and **E**).

It is also noteworthy that during the Tn to Te transition, 2,577 genes exhibited ≥ 2 fold changes in H3K4me3 and H3K27ac signals at promoters, 618 (24%) of which did not show an expression change. During Te to Tcm transition, 1,785 genes exhibited ≥ 2 fold changes in H3K4me3 and H3K27ac signals at promoters, 431 (24%) of which did not show an expression change. For these ~24% genes showing discordance, the activating histone marks might be cancelled out by counter-acting histone modifications, such as 1) bivalent modification, 2) regulation through other lysine or arginine residues, *e.g.,* H3K9 methylation, and/or 3) other forms of histone modifications including ubiquitination, sumoylation and/or phosphorylation. These same reasons might also explain discordance of active enhancers and their target genes, *i.e*., 2,529 genes exhibited ≥ 2 fold changes in H3K4me1 and H3K27ac signals at the regulating enhancers, 591 (23%) of which did not show an expression change during Te to Tcm transition; 2,363 genes exhibited ≥ 2 fold changes in H3K4me1 and H3K27ac signals at the regulating enhancers, 557 (24%) of which did not show an expression change during Te to Tcm transition.

He et al. Supplemental Figure 4

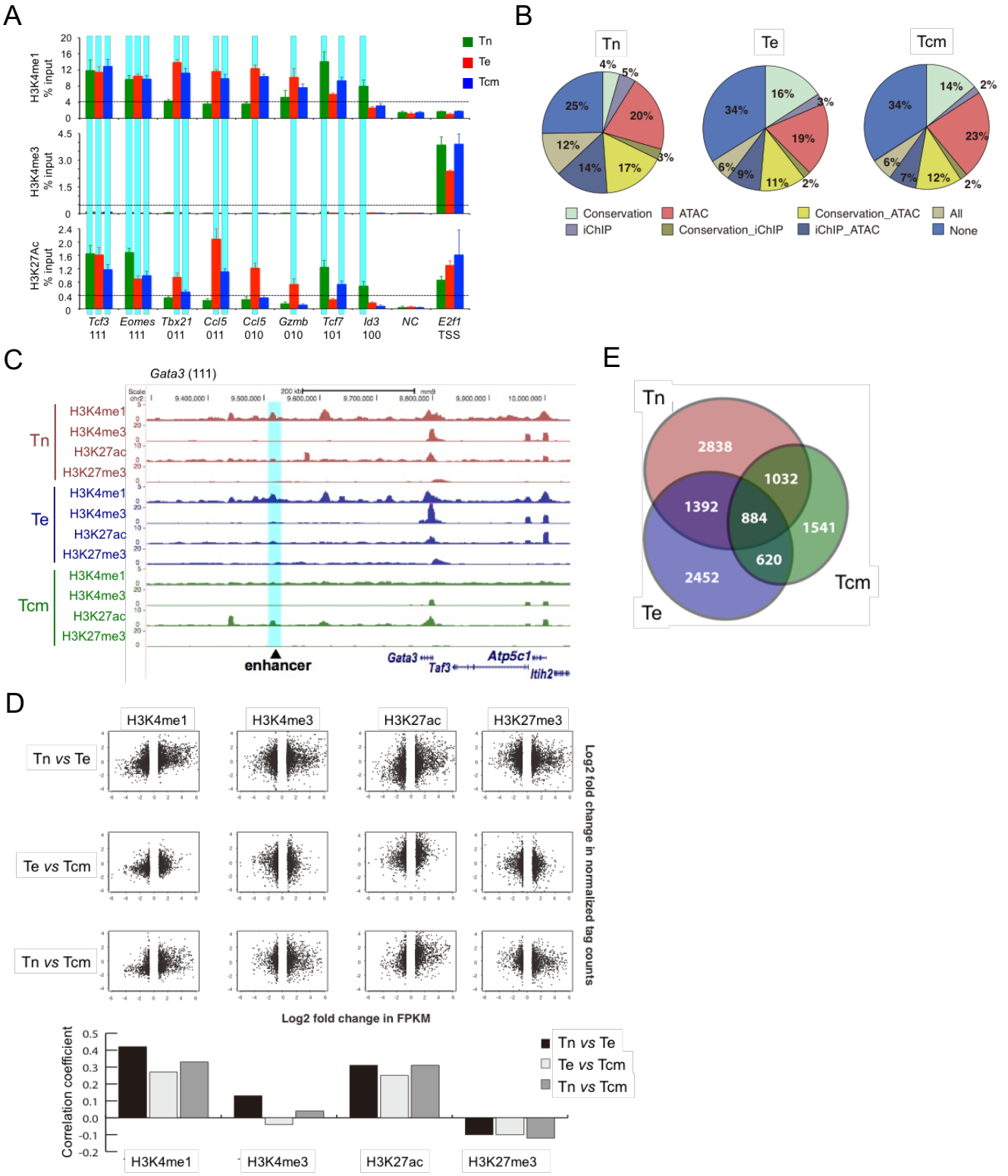

Figure S4 (related to Figures 2 and 3). Experimental and computational validation of predicated enhancers in CD8$^+$ T cell subsets.

(A) Validation of the histone mark features at predicted enhancers using Tn, Te, and Tcm cells collected after

bacterial infections. Naive OT-1 TCR Tg $CD8^+$ T cells (Tn) were isolated, then adoptively transferred into congenic mice followed by infection with *Listeria monocytogenes* expressing ovalbumin, and Te and Tcm were isolated on days 7 and ≥ 60 post-infection, respectively. ChIP was performed on each T cell population using anti-H3K4me1, anti-H3K4me3, and anti-H3K27ac antibodies. Two independent experiments were performed and each sample was measured by qPCR in duplicates.

The signal strength of each histone mark at select loci was determined in ChIP and input samples by quantitative PCR. The relative enrichment of a histone mark was calculated by normalizing signals in ChIP samples to those in input. Vertical cyan bars highlight the enhancers with confirmed histone mark features, *i.e.*, $H3K4me1^{hi}$, $H3K4me3^{lo}$, and $H3K27ac^{hi}$. The dotted lines mark empirically determined enrichment thresholds for different histone marks. NC, negative control genomic region that is devoid of histone modification signals based on the ChIP-Seq data. *E2f1* is expressed in $CD8^+$ T cells at all response stages and its transcription start site (TSS) was used as another control for low H3K4me1 signals and high H3K4me3 signals.

(B) Corroborating evidence for the predicted enhancers. Sequences of the predicted enhancers were examined for 1) conservation across 20 mammalian species; 2) overlap with Tn enhancers identified by iChIP or overlap with open chromatin regions determined by ATAC-Seq. Percentage of overlap of our predicted enhancers with one or more lines of corroborating evidence is shown. Details are summarized in **Table S4**. Conservation, sequence conservation across 20 mammalian species. iChIP, enhancers predicted using H3K27ac and H3K4me1 in *Lara-Astiago et al. Science 345, 943, 2014*. ATAC, open chromatin regions determined by ATAC-Seq in *Lara-Astiago et al. Science 345, 943, 2014*.

(C) Genome browser view of the previously identified *Gata3* enhancer. ChIP-Seq tracks at the *Gata3* locus are shown, and the known -280 kb enhancer is highlighted in cyan.

(D) Correlation between histone modification signals at active enhancers and expression levels of the target genes. Differentially expressed genes were identified through pair-wise comparison among the $CD8^+$ T cell subsets as described in **Figure 1**. Enhancer targets were predicted using the IM-PET algorithm. The histone mark tag counts changes at enhancer regions were then plotted against target gene expression changes for each pair-wise comparison among Tn, Te, and Tcm cells. Pearson correlation coefficient is shown in lower panel.

(E) Venn diagram of enhancer-promoter interactions using the nearest gene(s) of an enhancer as its target(s). Note that multiple enhancers can be found in the regulatory region of one gene, the numbers of target genes are lower than those of enhancers identified (compare with **Figure 2A**). The genomic locations of an enhancer and its nearest gene are listed in **Table S4**.

He et al. Supplemental Figure 5

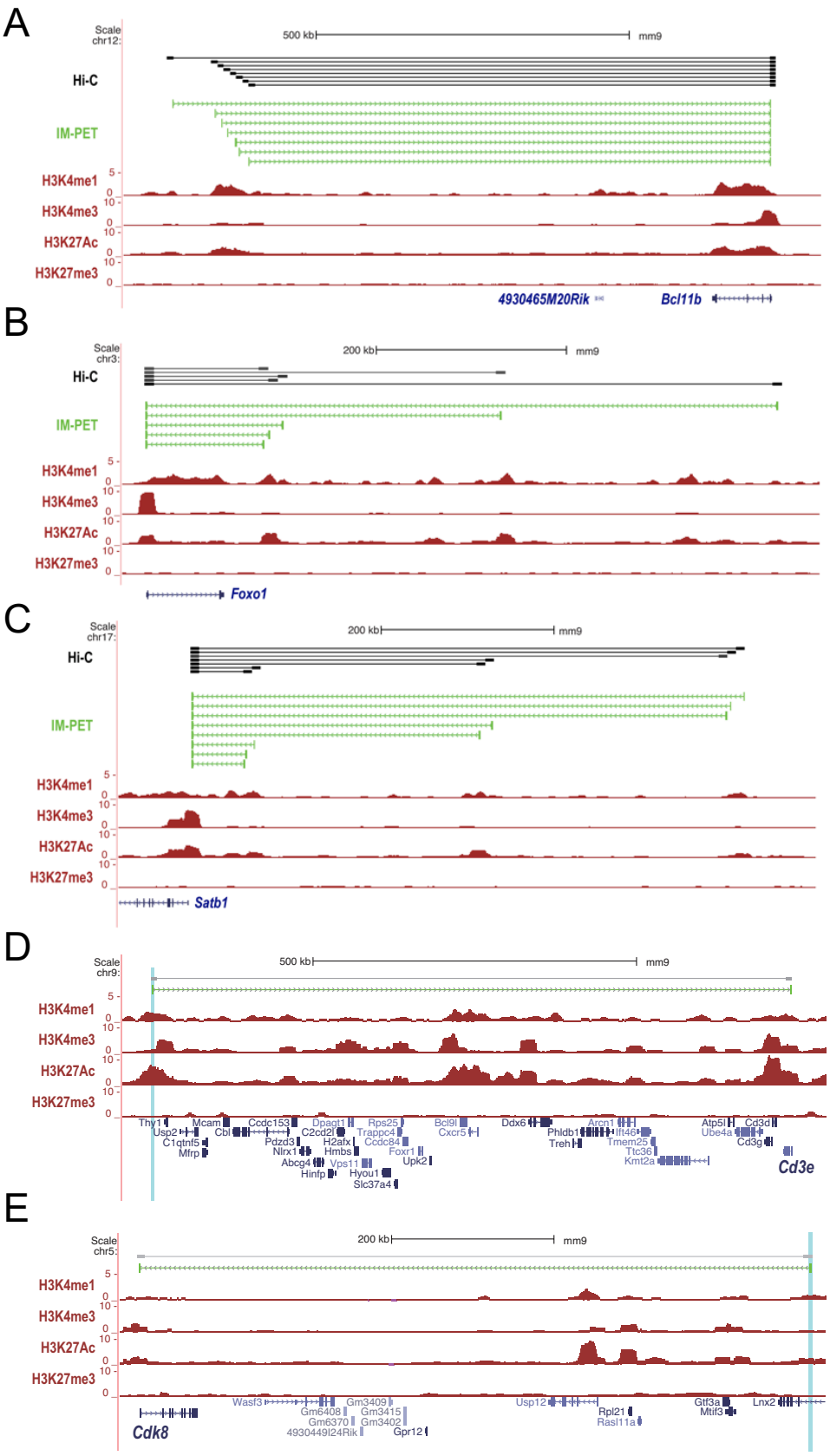

Figure S5 (related to Figure 3). Enhancer-promoter interactions predicted by IM-PET are supported by chromatin interactions detected by Hi-C. IM-PET-predicted and Hi-C-validated enhancer-promoter interactions at select gene loci in Tn cells. Shown are histone mark ChIP-Seq tracks at the *Bcl11b* (**A**), *Foxo1* (**B**), *Satb1* (**C**), *Cd3e* (**D**), and *Cdk8* (**E**) loci, with IM-PET-predicted interactions shown as green lines ending with bars. Hi-C interactions at 10 kb resolution are shown as grey lines ending with bars. The shades of grey denote statistical significance of the interaction, with darker shade indicating more significant interaction.

He et al. Supplemental Figure 6

A

	Th1 (724)	Th2 (682)	Th17 (877)
Tn (828)	269 (0.32)	176 (0.21)	281 (0.34)
Te (512)	160 (0.31)	98 (0.19)	175 (0.34)
Tcm (528)	229 (0.43)	149 (0.28)	220 (0.42)

B

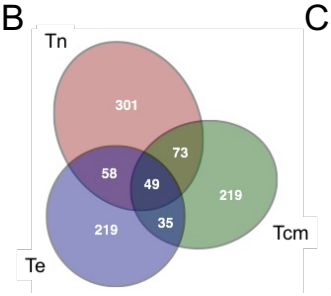

C

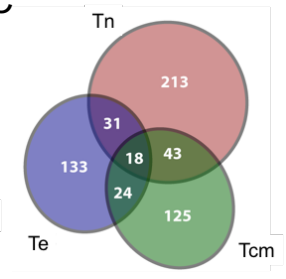

D

Super-enhancer activity	TCR signaling pathway (KEGG, DAVID, GO-term Signal transduction)		Other Kinases	
	non-DEGs	DEGs	non-DEGs	DEGs
N (100)	*Bcl10, Card11, Cd3e, Cd3g, Cblb Rasgrp1, Map3k7, Lat, Lck*	*Cd28 (ExpCluster 1) Itpkb (ExpCluster 10) Rac2 (ExpCluster 4)*	*Cdc42bpg, Cdk17, Map4k4 Pip4k2a, Rps6kb1, Sbk1 Snrk*	*Camk4 (ExpCluster 8) Srpk1 (ExpCluster 12)*
NE (110)	*Pik3cd*		*Mknk2, Eif2ak3, Cerk Stk10, Ern1, Sh3kbp1*	
NEM (111)	*Nck2, Prkcb*	*Fyn (ExpCluster 3) Pik3r5 (ExpCluster 3)*	*Clk2*	
NM (101)	*Cd3e, Cd3g, Cd3d, Itk, Grap2 Prkcq, Rras2*	*Ikbkb (ExpCluster 11)*	*Ptk2b, Nadk, Tssk6*	*Skp1a (ExpCluster 11)*
E (010)	*Calm2, Grb2, Prkcb, Raf1, Vav1*		*Camk2g, Map3k8, Pan3 Rps6kb1, Tbk1, Tbrg4*	
M (001)	*Cd8a, Cdc42, Pik3r1, Pik3r5, Plcg1 Nck2, Ptpc1, Map3k1*		*Stk11*	
EM (011)			*Ptk2b*	

E

Super-enhancer activity	Cytokine/Chemokine, receptors and siganling pathway		Cell adhesion and migration	
	non-DEGs	DEGs	non-DEGs	DEGs
N (100)	*Cxcr4, Ifnar1, Tgfbr2*		*Cd2, Celsr1, Itgb3, Gna13 Nisch, Myh9, Wasf2*	*Actn1 (ExpCluster 9)*
NE (110)		*Ifngr1 (ExpCluster 2)*	*Cd6, Icam2*	*Pecam1 (ExpCluster 10)*
NEM (111)			*B4galt1, Jak1*	
NM (101)	*Tnfrsf14*	*Ccr7 (ExpCluster 10)*	*Cyfip2, Cdh23, Myh9 S1pr1, Thy1*	*Sell (ExpCluster 10)*
E (010)		*Rasgrp2 (ExpCluster 5)*	*Pstpip1*	*Adam8 (ExpCluster 4) Cerkl (ExpCluster 2) Itgal (ExpCluster 3) Itgam (ExpCluster 3) Pkp4 (ExpCluster 10)*
M (001)	*Clcf1*	*Il10ra (ExpCluster 3)*		
EM (011)	*Ifnar1*	*Ccl3 (ExpCluster 3) Ccl5 (ExpCluster 3) Ccl6 (ExpCluster 4) Ccl9 (ExpCluster 4) Il10rb (ExpCluster 1) Ifnar2 (ExpCluster 6)*		

F

Super-enhancer activity	TFs and other factors regulating transcription	
	non-DEGs	DEGs
N (100)	*Bcl11b, Chd7, Elf1, Elk3, Ets1, Hivep2, Ikzf1 Irf9, Kdm5a, Klf13, Mbd2, Ncoa2, Ncoa3 Nfatc2ip, Nfkb1, Nfe2l2, Pbrm1, Pnrc2, Rb1 Rest, Tsc22d4, Zkscan1, Zkscan5*	*Bach (ExpCluster 10) Gtf2i (ExpCluster 10) Lef1 (ExpCluster 9) Nrip1 (ExpCluster 9) Rere (ExpCluster 9) Smad3 (ExpCluster 2) Zfp1 (ExpCluster 11)*
NE (110)	*Foxk1, Tcf3, Vgll4, Bptf, Ets1*	
NEM (111)	*Arid1a, Bcl11b, Ikzf1*	*Ikzf3 (ExpCluster 3) Irf1 (ExpCluster 5) Zmiz1 (ExpCluster 4)*
NM (101)	*Arid5a, Runx3, Nfatc1, Taf8*	*Tcf7 (ExpCluster 10)*
E (010)	*Hmga1, Irf2, Runx3, Mta1, Eaf1, Arf7ip Sp4, Trerf1, Zfp511, Zfp263, Znfx1*	*Ssbp3 (ExpCluster 8) Tcfeb (ExpCluster 5)*
M (001)	*Ascc1, Ilf3, Kat5, Med29 Mef2d, Paf1, Sp2*	*Fos (ExpCluster 10) Smad7 (ExpCluster 10) Rara (ExpCluster 4 Rora (ExpCluster 3) Pias (ExpCluster 4)*
EM (011)	*Taf1c, Nfatc2*	

Figure S6 (related to Figure 5). Super enhancers and their target genes in $CD8^+$ T cell subsets.

(A) Super enhancer overlap between $CD4^+$ and $CD8^+$ T cells. $CD4^+$ T cell super enhancers were retrieved from Vahedi G *et al*. Fractional numbers are the ratio of the number of shared SEs over the total number of SEs in a given $CD8^+$ T cell subset.

(B) Venn diagram for super enhancer targets in three $CD8^+$ T cell subsets. We assigned a gene as a super enhancer target if it was predicted to be targeted by 50% or more of the member enhancers of the super enhancer. Enhancer targets were predicted using the IM-PET algorithm.

(C) Venn diagram for nearest genes of super enhancers in three $CD8^+$ T cell subsets. The genome locations of a super enhancer and its nearest gene are listed in **Table S6**.

(D-F) Functional annotation of super enhancer target genes. The target genes were analyzed using the DAVID bioinformatics resource and KEGG pathway tool. The prominent functional categories were summarized, with "T cell signaling pathway" and "kinases" in (**D**), "cytokine, chemokine and their receptors", "cell adhesion" and "cell migration" in (**E**), and "transcription factors" and other factors under "regulation of transcription" in (**F**). Both non-DEGs and DEGs are listed, and the ExprCluster membership is also marked for the DEGs.

He et al. Supplemental Figure 7

A

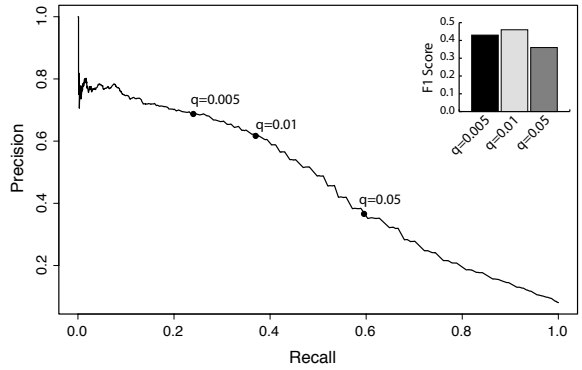

B

Stage-specificity	Transcription Factor
Tn (28)	*CTCF, EGR1, ESRRA, FLI1, FOXJ2, FOXJ3, GATA3, IRF1, IRF3, LEF1, MEF2A, MTF1, NF1, RFX2, RFX3, RORA, RREB1, RUNX3, SF1, SMAD4, SP2, SRF, STAT3, TCF12, TCF7, ZFP187, ZFP281, ZFP740*
Te (14)	*BACH1, EOMES, MGA, JDP2, KLF4, KLF7, LMO2, NFE2, NR2F6, RARA, RXRA, SMAD3, TBX21, TCF3*
Tcm (18)	*ATF1, CTCF, EGR1, FOXO1, GABPA, KLF16, KLF6, REST, RREB1, RXRB, SP1, SP2, STAT5A, TCF7, ZFP281, ZFP740, ZFX, ZIC1*
Tn & Te (11)	*E2F3, ELF2, FOXO3, HSF1, JUNB, MAX, NFKB2, RARG, RELA, ZFX, ZFP691*
Tn & Tcm (5)	*ATF7, HOMEZ, IRF2, NFYA, PRDM4*
Te & Tcm (11)	*ARNT, ELF1, ETV3, GABPB, KLF13, MLX, MXI1, NFAT5, PRDM1, THRA, ZBTB7B*
Tn, Te, & Tcm (7)	*KLF4, LMO2, MNT, SFPI1, SPIC, TCF4, ZFX*

C

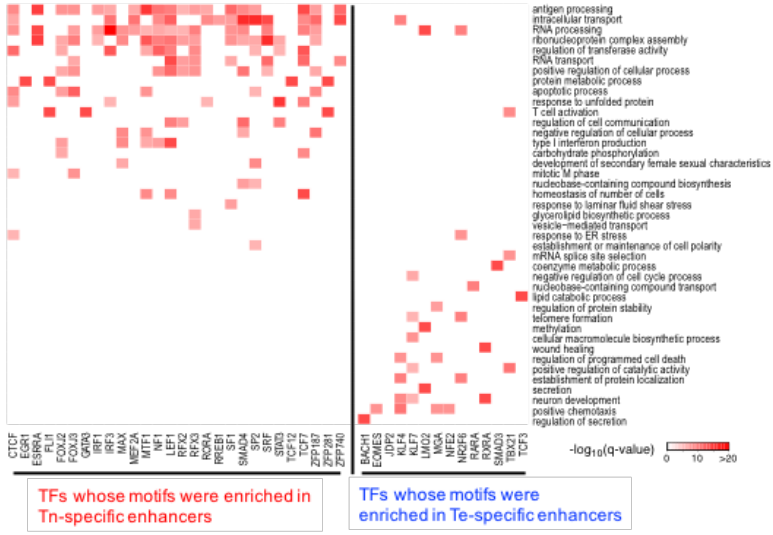

D

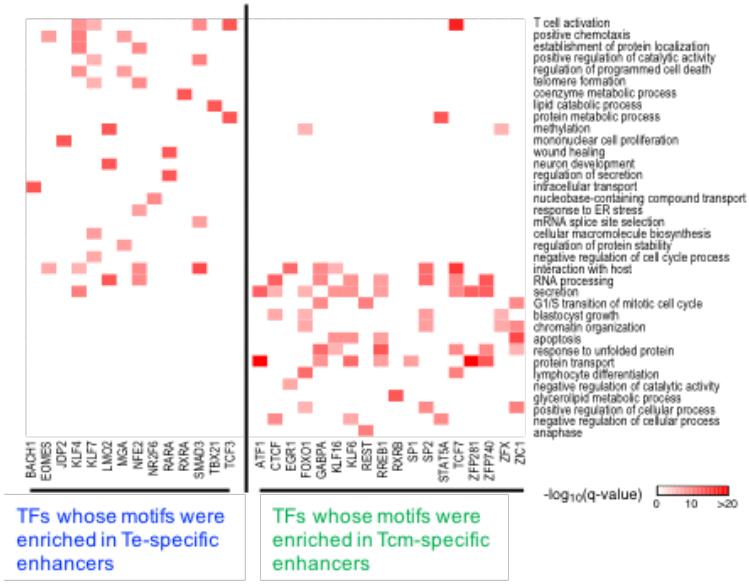

Figure S7 (related to Figures 6 and 7). Transcription regulatory networks during CD8$^+$ T cell responses.

(A) Precision and recall curve for identifying TF binding sites in enhancers. TF binding sites (TFBS) within enhancer sequences were identified using FIMO at different q-values. To evaluate the accuracy of TFBS prediction, we collected a set of 4 TF ChIP-Seq data (Tcf1, Gata3, Fli1, and Runx3) performed on Tn cells. TF ChIP-Seq peaks were treated as the gold standard TFBSs. Recall was defined as the fraction of ChIP-Seq peaks that overlap with enhancers containing predicted binding sites by the same TF. Precision was defined as the fraction of enhancers containing predicted binding sites that overlap with ChIP-Seq peaks by the same TF. F1 score was defined as the harmonic mean of precision and recall.

(B) Transcription factors whose DNA binding motifs were enriched at stage-specific enhancers. Values in parentheses denote the number of TFs at each stage. TFs highlighted in blue are identified in enhancers that are active in ≥ 2 stages.

(C) Functional annotation of TF-target genes in Tn and Te cells. TF motifs enriched in Tn or Te-specific enhancers were identified, and for each TF, its predicted stage-specific target genes in Tn or Te cells were analyzed for enriched GO terms. GO term enrichment p-value was computed using the hypergeometric distribution. Color shade is proportional to the statistical significance of the enrichment.

(D) Functional annotation of TF-target genes in Te and Tcm cells. TF motifs enriched in Te or Tcm-specific enhancers were identified, and for each TF, its predicted stage-specific target genes in Te or Tcm cells were analyzed for enriched GO terms. Color shade is proportional to the statistical significance of the enrichment.